An α7 Nicotinic Acetylcholine Receptor Gain-of-Function Mutant That Retains Pharmacological Fidelity

Andon N. Placzek, Francesca Grassi, Edwin M. Meyer, and Roger L. Papke

Department of Pharmacology and Therapeutics, University of Florida, Gainesville, Florida (A.N.P., E.M.M., R.L.P.); and Istituto Pasteur-Fond. Cenci Bolognetti and Dipartimento di Fisiologia Umana e Farmacologia, Università degli Studi di Roma "La Sapienza", Rome, Italy (F.G.)

Received July 1, 2005; accepted September 23, 2005

ABSTRACT

The α7-type nicotinic acetylcholine receptor (nAChR) has been recognized as a potential therapeutic target for the treatment of a variety of pathologic conditions, including schizophrenia, Alzheimer's disease, and peripheral inflammation. A unique feature of α7 nAChRs that tends to complicate functional assays intended to identify selective drugs for these receptors is the strong concentration-dependent desensitization of their agonist-evoked responses. At low agonist concentrations, voltage-clamp responses are small but tend to closely follow the solution exchange profile, whereas higher agonist concentrations produce responses that peak and then decay very rapidly, usually before the full drug concentration has been achieved. In this article, we report that an α7 T245S mutant, which has a point mutation at the sixth position in the α7 second transmembrane domain (T6′S), demonstrates a significant gain of function, sustaining current when exposed to relatively high agonist concentrations when expressed in *Xenopus laevis* oocytes and larger peak currents when expressed in mammalian GH4C1 cells. At the single-channel level, the T6′S mutant has a unitary conductance of 61.7 ± 5.8 pS, similar to that reported for wild-type α7, but a vastly longer average open duration. In addition, channel burst activity indicates a greater than 40% probability of channel re-opening in the sustained presence of 30 μM acetylcholine, consistent with a greater overall open probability relative to wild-type α7. Unlike the α7 L248T gain-of-function mutant, the T6′S mutant exhibits a pharmacological profile that is remarkably similar to the wild-type α7 receptor, implicating it as a potentially useful tool for identifying therapeutic agents.

Nicotinic acetylcholine receptors (nAChR) composed of the α7 subunit are pentameric, ligand-gated ion channels that are widely expressed in mammalian tissues, including both central and peripheral neurons (Dani, 2001; Skok, 2002), as well as non-neuronal cells (Wang et al., 2003; Shytle et al., 2004). Although the normal physiological functions of α7-type nAChRs are poorly understood, studies have shown behavioral effects of α7-selective agonists suggesting a role in learning and memory function (Rezvani and Levin, 2001). Other reports have implicated α7 nAChRs as potential therapeutic targets in schizophrenia (Freedman et al., 2000) and neurodegenerative conditions such as Alzheimer's disease (O'Neill et al., 2002). Recent studies have also shown that α7 receptors play an important role in peripheral inflammatory processes (Wang et al., 2003), suggesting that selective targeting of α7 nAChRs may be beneficial in preventing the deleterious effects of septicemia.

The α7-type nAChRs are unique among nicotinic receptors in that they display a high degree of concentration-dependence to the kinetics of agonist-evoked responses. That is, with the application of increasing concentrations of agonist, the macroscopic responses of α7 nAChRs become more and more transient, to the point where the peak of the response occurs well before the maximum concentration is achieved (Papke and Thinschmidt, 1998). This is true even for very rapid drug application systems, indicating that the macroscopic kinetics of wild-type α7 receptors are faster than the rate of currently available agonist application devices (Papke et al., 2000a; Uteshev et al., 2002). The fact that α7 nAChRs have been reported to have a very high permeability to calcium (Seguela et al., 1993) suggests that this agonist concentration-dependent limitation of the channel's activity may help prevent excitotoxic injury in cells with high levels of α7 receptors expressed (Li et al., 1999).

Previous work in our laboratories has shown that the 6′

ABBREVIATIONS: nAChR, nicotinic acetylcholine receptor; TM2, second transmembrane domain; ACh, acetylcholine; KRH, Krebs-Ringer-HEPES; 5HI, 5-hydroxyindole; P_{fCa}, Ca^{2+} fractional permeability; P_{open}, open probability; CRC, concentration-response curve; GTS-21, (2,4)-dimethoxybenzylidene anabaseine dihydrochloride; AR-R17779, (−)-spiro[1-azabicyclo[2.2.2]octane-3,5′-oxazolidin-2′-one].

position of the pore-forming, second transmembrane (TM2) domain [according to the numbering scheme proposed by Miller (1989)] is an important regulator of several features that distinguish major subfamilies of nAChR (Webster et al., 1999; Placzek et al., 2004). This site corresponds to amino acid 245 in the rat α7 nAChR sequence. In an earlier study of α7, the wild-type threonine residue was substituted with a phenylalanine residue at position 245 of the rat α7, resulting in a T6'F mutant (Placzek et al., 2004). Receptors containing this mutation generated only small currents; however, these currents lacked the agonist concentration-dependent kinetic effects characteristic of wild-type α7. In addition, the T6'F mutant displayed some pharmacological properties that are like the muscle-type nAChR (Placzek et al., 2004). In an effort to test whether an analogous effect could be produced with a similar single amino acid substitution in the α7 TM2 domain, an α7 T6'S mutant was constructed. In this case, the α7 wild-type threonine at position 245 of the rat α7 was exchanged for the serine residue present at the homologous position of the neuronal $\beta2/\beta4$ subunit (see Fig. 1), yielding a T6'S mutant α7.

As in the case of the T6'F mutant, much of the rationale for the hypothesized effects of the T6'S mutant are derived from previously published observations with heteromeric nAChRs. For example, sensitivity to the ganglionic blocker mecamylamine was increased in muscle-type receptors with chimeric $\beta1(\beta4)$ subunits, and this effect could be attributed to the sequence differences at the TM2 6' and 10' positions (Webster et al., 1999).

In characterizing the effects of this TM2 T6'S mutation, we describe a mutant receptor that retains much of the pharmacology of wild-type α7, but with larger macroscopic responses and a dramatic lessening of agonist concentration-dependent limitation on response duration. The effects of this mutation are examined at the single-channel level and indicate that channel open time and burst properties are affected, rather than receptor expression, or single-channel conductance. Furthermore, the T6'S α7 mutant displays a pharmacological profile that is very similar to that of wild-type α7. A gain-of-function mutant that retained much of the pharmacology of the wild-type receptor would have significant utility for drug development.

Materials and Methods

cDNA Clones. These experiments used rat neuronal nAChR cDNA clones, which were obtained from Dr. Jim Boulter (University of California, Los Angeles, CA). The sequences of the TM2 domains of the relevant subunits are shown in Fig. 1. The 20 residues in the putative second transmembrane sequence are identified as 1' through 20' (Miller, 1989).

Site-Directed Mutagenesis. Site-directed mutagenesis was performed using QuikChange kits (Stratagene, La Jolla, CA). In brief,

two complimentary oligonucleotides were synthesized that contained the desired mutation flanked by 10 to 15 bases of unmodified nucleotide sequence. Using a thermal cycler, *Pfu* DNA polymerase extended the sequence around the whole vector, generating a plasmid with staggered nicks. Each cycle built only off the parent strands, and therefore there was no amplification of misincorporations. After 12 to 16 cycles, the product was treated with DpnI, which digested the methylated parent DNA into numerous small pieces. The product was then transformed into *Escherichia coli* cells, which repaired the nicks.

Preparation of RNA. After linearization and purification of cloned cDNAs, RNA transcripts were prepared in vitro using the appropriate mMessage mMachine kit from Ambion Inc. (Austin, TX).

Expression in *Xenopus laevis* Oocytes. Mature (>9 cm) female *X. laevis* African frogs (Nasco, Ft. Atkinson, WI) were used as a source of oocytes. Before surgery, frogs were anesthetized by placing the animal in a 1.5 g/l solution of MS222 (3-aminobenzoic acid ethyl ester). Oocytes were removed from an incision made in the abdomen.

To remove the follicular cell layer, harvested oocytes were treated with collagenase from Worthington Biochemical Corporation (Freehold, NJ) for 2 h at room temperature in calcium-free Barth's solution (88 mM NaCl, 1 mM KCl, 15 mM HEPES, pH 7.6, 0.81 mM MgSO$_4$, 2.38 mM NaHCO$_3$, and 0.1 mg/ml gentamicin sulfate). Thereafter, stage 5 oocytes were isolated and injected with 5 to 10 ng each of the appropriate subunit cRNAs after harvest. Recordings were made 3 to 14 days after injection depending on the cRNAs being tested. Because all data were normalized using each cell as its own control, absolute differences in response magnitude did not affect comparisons between receptor subtypes.

Voltage-Clamp Recording of Oocyte Responses. Data were obtained by means of two-electrode voltage-clamp recording. Recordings were made at room temperature (21–24°C) in Frog Ringer's solution (115 mM NaCl, 10 mM HEPES, 2.5 mM KCl, and 1.8 mM CaCl$_2$, pH 7.3) with 1 μM atropine to inhibit muscarinic acetylcholine receptor responses. This extracellular solution was used for all experiments unless otherwise noted. Voltage electrodes were filled with 3M KCl, and current electrodes were filled with 250 mM CsCl, 250 mM CsF, and 100 mM EGTA, pH 7.3.

Bath solution and drug applications were applied through a linear perfusion system to oocytes placed in a Lucite chamber with a total volume of 0.5 ml. Drug delivery involved preloading 1.8 ml of tubing at the terminus of the perfusion system, while a Mariotte flask filled with Ringer's solution was used to maintain constant perfusion. Applications of drug solutions were then synchronized with acquisition. Current responses were recorded using a PC interfaced to either a Warner OC-725C (Warner Instruments, Hamden, CT) or a GeneClamp 500 amplifier via a Digidata 1200 digitizer (Molecular Devices, Sunnyvale, CA). In addition, some oocyte recordings were made using a beta version of the OpusXpress 6000A (Molecular Devices). OpusXpress is an integrated system that provides automated impalement and voltage clamp of up to eight oocytes in parallel. Cells were automatically perfused with bath solution, and agonist solutions were delivered from a 96-well compound plate. In experiments using the OpusXpress system, the voltage and current electrodes were filled with 3 M KCl. In all experiments, bath flow rates were set at 2 ml/min.

Current responses to drug application were studied under two-

Fig. 1. Amino acid sequences for wild-type and the T6'S mutant α7 nAChR TM2 domains based on the numbering of specific residues of the second membrane-spanning region (Miller, 1989). The corresponding sequences for neuronal β subunits are also given as a reference. The 6' position is indicated by the box.

electrode voltage clamp at a holding potential of −50 mV unless otherwise noted (−60 mV for the OpusXpress system). Holding currents immediately before agonist application were subtracted from measurements of the peak to agonist. All drug applications were separated by wash periods of 5 min unless otherwise noted. At the start of recording, all oocytes received two initial control applications of ACh. Subsequent drug applications were normalized to the second acetylcholine application to control for the level of channel expression in each oocyte. Means and standard errors (S.E.M.) were calculated from the normalized responses of at least four oocytes for each experimental concentration.

For concentration-response relations, data were plotted using Kaleidagraph 3.0.2 (Abelbeck Software; Reading, PA), and curves were generated using the equation Response = $(I_{max} [\text{agonist}]^{n_H})/([\text{agonist}]^{n_H} + (EC_{50})^{n_H})$, where I_{max} denotes the maximal response for a particular agonist/subunit combination and n_H represents the Hill coefficient. I_{max}, n_H, and the EC_{50} were all unconstrained for the fitting procedures.

Calculations of peak amplitudes and net charge were made using pClamp either during acquisition or during subsequent Clampfit analysis. Note that measurement of net charge has been shown to be a more accurate indicator of fast responses of wild-type α7 than measurement of peak response (Papke and Papke, 2002). Baseline was defined for Clampfit statistics as 20 s before drug application, and the analysis region for peak and net charge analysis went from 5 s before the initiation of drug application and extended at least 135 s after. Area analysis data are provided for all receptor subtypes examined in this article for comparison with wild-type α7.

Transfection and Patch-Clamp Recording from GH4C1 Cells. GH4C1 cells were cultured in F10 medium (Invitrogen, Carlsbad, CA) at 37°C, 5% CO_2. Cells were transiently transfected using Fugene (Roche, Indianapolis, IN) according to the manufacturer instructions. One microgram of wild-type or T6'S mutant α7 cDNA in the pCIneo vector (Promega Corp., Madison WI) was added to each 35-mm Petri dish, together with 0.5 or 1 μg of the cDNA encoding the red fluorescent DsRed protein (BD Biosciences Clontech, Palo Alto, CA). Cells were used 48 to 72 h after transfection. Typical transfection efficiency was 10 to 25% using this method.

Whole-Cell and Fluorescence Measurements in GH4C1 Cells. ACh-evoked currents and fluorescence measurements were simultaneously performed on cells loaded with Fura-2 (Molecular Probes, Eugene, OR) via the patch pipette. Whole-cell currents were recorded using an Axopatch 200B amplifier (Molecular Devices) at room temperature. Cell were bathed in a solution containing 140 mM NaCl, 3 mM KCl, 2 mM $CaCl_2$, 2 mM $MgCl_2$, 10 mM glucose, and 10 mM HEPES/NaOH, pH 7.3. Patch electrodes (tip resistance, 3–5 MΩ) were filled with 140 mM N-methylglucamine, 10 mM HEPES/HCl, pH 7.3, plus 250 μM Fura-2. Cells were continuously superfused by a gravity-driven fast-exchanging perfusion system (RSC 200; BioLogic, Grenoble, France), with independent tubes for each solution placed approximately 100 μm from the cells. Currents were recorded at 2 kHz using pClamp 8 and a membrane holding potential of −70 mV unless otherwise indicated. Analysis was performed using pClamp 8.

Fluorescence determinations were made using a Zeiss Axioskop 2 FS microscope (Germany) equipped with a monochromator (Optoscan, Cairn, UK) and a high-sensitivity digital camera (SensiCam; PCO, Kelheim, Germany). The Axon Instrument Workbench 2 was used for data sampling and analysis. Fluorescence values were averaged over domains approximating the cell shape, assuming a homogeneous receptor density. Cells were loaded with fura-2 in the whole-cell configuration, until the basal fluorescence (F_0) reached a stable value (usually 3–5 min). The so-called "F/Q ratio" was determined as the ratio of the fluorescence change ($\Delta F/F_0$) at the excitation wavelength of 380 nm over the total charge (Q) entering the cell. The F/Q ratio was calculated as the slope of the line fitting F versus Q points, taking into account only the data within 600 ms of transmitter application, when Ca^{2+} extrusion can be assumed to be neg-

ligible (Bollmann et al., 1998) and the relationship is indeed linear. Fractional Ca^{2+} permeability (P_f) was obtained by normalizing the F/Q ratio obtained in standard medium (containing 2 mM Ca^{2+}) to the F/Q ratio measured in calibration experiments, when Ca^{2+} is the only permeant cation. To this purpose, cells were bathed in a solution containing 130 mM N-methylglucamine, 10 mM $CaCl_2$, 10 mM HEPES/HCl, pH 7.3. Cells displaying high basal F_{340}/F_{380} ratio values (>1 in our conditions) or low basal F_{380} values (<150 arbitrary units in our conditions) were not considered for analysis. Experimental procedures and data analyses were as described previously (Ragozzino et al., 1998). Chemicals were purchased from Sigma Chemical (St. Louis, MO).

Single-Channel Patch Clamp Recordings from Transfected GH4C1 Cells. Single-channel currents were recorded in the cell-attached patch configuration using an Axopatch 200A amplifier (Molecular Devices) at room temperature. Cells were bathed in a solution containing 140 mM NaCl, 2.8 mM KCl, 1 mM $CaCl_2$, 1 mM $MgCl_2$, 10 mM glucose, 10 mM HEPES/NaOH, pH 7.3. Patch electrodes (tip resistances, 5–7 MΩ after fire polishing) were coated with Sylgard (Dow Corning, Midland, MI) and filled with the same extracellular solution plus 1 μM atropine and 30 μM ACh. Currents were filtered at 10 kHz and digitized at 50 kHz using pClamp 8 (Molecular Devices). Analysis was conducted using pClamp 9.

Radioligand Binding Studies. GH4C1 cells were harvested from 60-mm culture dishes using a sterile cell scraper and assayed for nicotine-displaceable, high-affinity [³H]methyllycaconitine binding using a modification of the procedure of Davies et al. (1999). Cells were suspended in 20 volumes of ice-cold Krebs-Ringer-HEPES (KRH; 118 mM NaCl, 5 mM KCl, 10 mM glucose, 1 mM $MgCl_2$, 2.5 mM $CaCl_2$, and 20 mM HEPES, pH 7.5). After two 1-ml washes with KRH at 20,000g, the membranes were incubated in 0.5 ml of KRH with 1, 3, 10, or 20 nM [³H]methyllycaconitine (Tocris, Ellisville, MO) for 60 min at 4°C with or without 5 mM nicotine. Tissues were washed three times with 5 ml of cold KRH by filtration through Whatman GF/C filters that had been preincubated for 2 h in bovine lacto-transfer optimizer (KRH with 0.5% dry milk and 0.002% sodium azide). They were then assayed for radioactivity using liquid scintillation counting. Inhibition curves generated under two-electrode voltage-clamp with oocytes expressing either wild-type α7 or the TM2 T6'S mutant showed a less than 3-fold difference in methyllycaconitine potency between the two (data not shown).

Intact Oocyte Binding. [³H]MLA binding in intact oocytes was performed similarly to the method described previously (Placzek et al., 2004). In brief, whole *Xenopus laevis* oocytes that were either uninjected or had been injected with mRNAs encoding either wild-type α7 or the T6'S mutant were placed in a single well of a 96-well plate containing either 20 nM [³H]methyllycaconitine alone or 20 nM [³H]methyllycaconitine with 5 mM nicotine. After four 4-s washes in 2.5 ml of KRH, total radioactivity was measured using an automated liquid scintillation counter as counts per minute. Nicotine displaceable binding was calculated for at least four cells in each condition.

Results

Effects of the TM2 T6'S Mutation on the Macroscopic ACh-Evoked Currents. Compared with the wild-type α7 (Fig. 2A) (Placzek et al., 2004), the α7 T6'S mutant showed a significant change in response kinetics to ACh, with currents somewhat slower to rise and of longer duration at high agonist concentrations. Figure 2 also shows the decreased effect of increasing concentrations of acetylcholine on the macroscopic decay rate of the T6'S mutant responses (Fig. 2B) compared with wild-type α7 (Fig. 2A) with its characteristically strong concentration-dependent kinetics. An analysis of the rise times (Fig. 2C) of these responses showed that the T6'S mutant actually exhibits a slowing of the response with increasing agonist concentration before the eventual increase

in rise time dominates at the highest concentrations. This is particularly true for acetylcholine concentrations of approximately 30 μM. The decay times of the T6'S mutant responses, much like those of the T6'F mutant (Placzek et al., 2004), showed little effect of high agonist concentrations, whereas the decay times of wild-type responses became progressively shorter at higher agonist concentrations (Fig. 2D).

A comparison of [³H]MLA binding between intact oocytes expressing either wild-type α7 or the T6'S mutant showed that the average difference in nicotine-displaceable binding was not statistically significant (Table 1). Despite this similarity in receptor binding, the ACh-evoked currents in cells

from the same injection set differed substantially in the amount of net charge. Currents from oocytes expressing either wild-type α7 or the T6'S mutant, all of which received mRNA injections on the same date, approximately 72 h before recording, indicated that the total area under the curve for the averaged wild-type α7 current was 11.5% of that of the T6'S mutant, a difference that cannot be attributed to differences in receptor expression (Table 1).

Ca²⁺ Permeability of α7 T6'S Mutant Receptors. The GH4C1 cell line has previously been shown to functionally express transfected wild-type α7 receptors at levels higher than other commonly used mammalian cell expression sys-
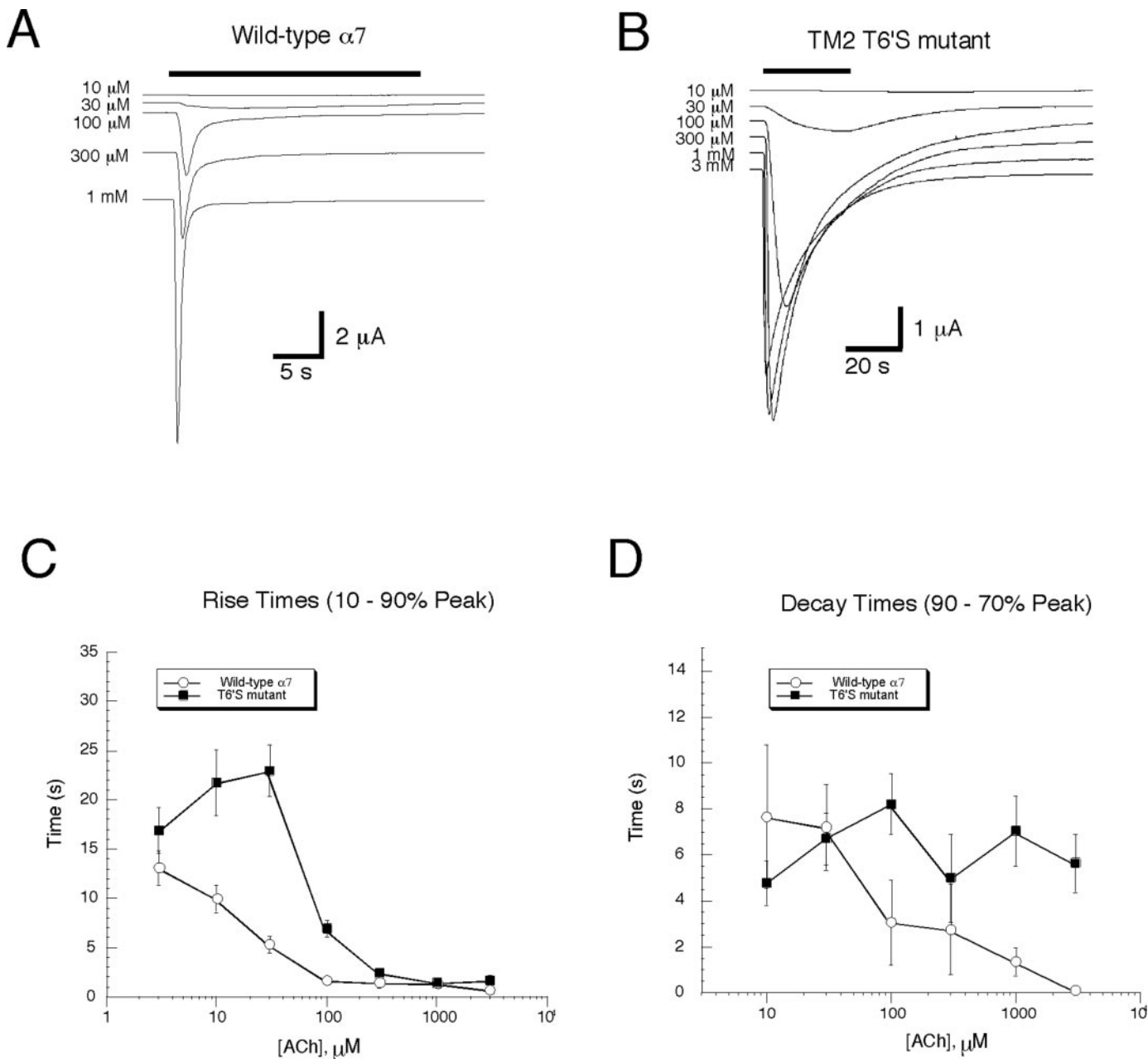

Fig. 2. The time course and concentration-dependence of α7 nAChR macroscopic kinetics are altered by the T6'S mutation. Two-electrode voltage clamp responses from oocytes expressing wild-type α7 (A), or the T6'S mutant (B). The traces show the relative effect of increasing concentrations of ACh. The T6'S mutant responses are slower and the effect of higher concentrations of agonist on the macroscopic kinetics reaches a maximum, whereas for wild-type α7, no maximum is achieved. C, the T6'S mutant shows a slowing of the rise time near 30 μM before the higher agonist concentrations dominate. D, the decay times also show that the T6'S mutant is insensitive to higher agonist concentrations, whereas the wild-type decay times become increasingly rapid. The wild-type data (A and C) were published previously (Placzek et al., 2004).

tems (Sweileh et al., 2000). The wild-type receptors heterologously expressed in this cell line have also been shown to have a high degree of pharmacological similarity to native α7

TABLE 1

Intact oocyte [³H]methyllycaconitine binding

Data are presented as mean counts per minute per cell ± S.E.M. for the indicated treatments.

	Binding
	cpm / cell (n)
Rat α7 wild-type	
20 nM MLA alone	143 ± 4 (5)*
20 nM MLA + 5 mM nicotine	100 ± 12 (4)
Rat α7 T6'S mutant	
20 nM MLA alone	169 ± 10 (5)*
20 nM MLA + 5 mM nicotine	106 ± 6 (5)
Uninjected oocytes	
20 nM MLA alone	98 ± 17 (4)

MLA, methyllycaconitine.

* $P \leq 0.05$ by Student's *t* test compared with the same receptor subtype in the presence of 20 nM methyllycaconitine with 5 mM nicotine.
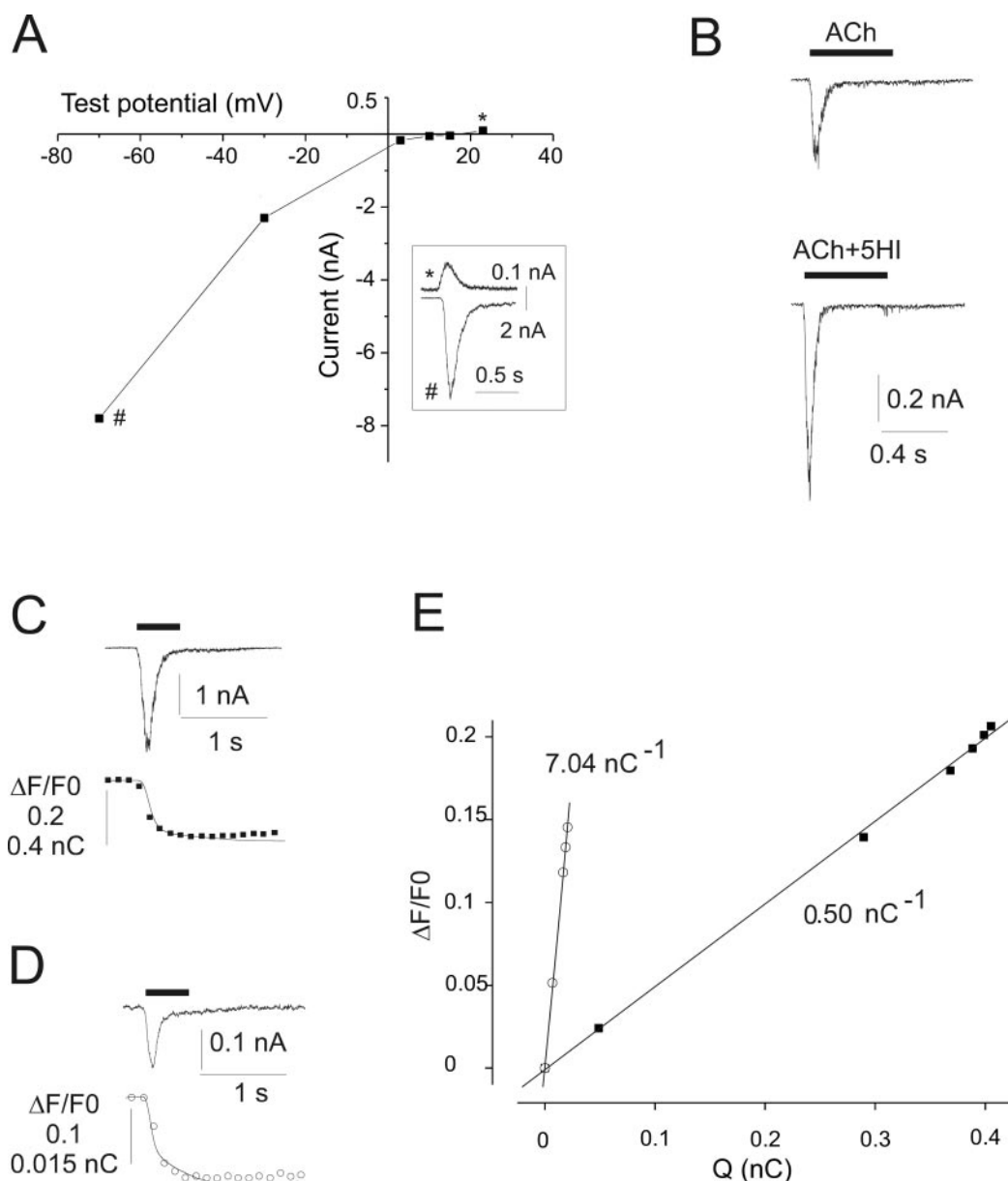
receptors expressed in rat brain (Quik et al., 1996), indicating GH4C1 cells as useful for studying α7-type nAChRs in small mammalian cells. GH4C1 cells successfully cotransfected with wild-type or the T6'S mutant α7 nAChR and DsRed protein showed a bright red fluorescence when excited at 550 nm. ACh-evoked currents in both wild-type (data not shown) and T6'S α7-expressing cells (Fig. 3A) showed a marked rectification of the current evoked at positive membrane potentials. However, acetylcholine elicited whole-cell currents (I_{ACh}) with much larger peak amplitude in cells expressing T6'S α7 nAChR than wild-type α7 nAChR ($p <$ 0.01, Table 2). Addition of 5-hydroxyindole (5HI) increased the peak amplitude of I_{ACh} ACh-evoked currents in wild-type and T6'S α7-expressing cells without affecting current rise and decay times (Fig. 3B). However, this potentiating effect of 5-hydroxyindole was significantly less ($p < 0.05$) for the T6'S mutant receptor than for wild-type α7 nAChR (Table 2). By contrast, ACh-evoked currents recorded from oocytes expressing T6'S mutant α7 receptors showed only a relatively

Fig. 3. Whole-cell current and Ca^{2+} determinations in GH4C1 cells expressing T6'S α7 nAChR. A, I_{ACh} recorded in a single cell, in the presence of 5HI, at different test potentials. Inset, currents recorded at -70 mV (#) or $+ 23$ mV (*). B, typical ACh-evoked current responses recorded in the same cell with or without 5HI, as indicated. Test potential -70 mV, [ACh] = 200 μM. C, simultaneous recordings of whole-cell current and Ca^{2+} responses elicited by acetylcholine (100 μM, $- 70$ mV) in standard medium. Top, I_{ACh}; bottom, fluorescence intensity, expressed as $\Delta F/F$ (■) and current integral (line). D, as in C, but in a different cell, bathed in calibration medium (10 mM Ca^{2+} as the only permeant cation). E, relationships between the fluorescence variation and the charge Q, fitted by linear regressions, from the same cells as in C (slope = 0.5 nC^{-1}) and D (slope = 7.04 nC^{-1}). The Pf for the T6'S α7 nAChR was 7.1%.

slight potentiation by 5HI. The small but significant ($p < 0.05$) 26% potentiation observed was dramatically lower than the average potentiation of wild-type $\alpha7$ receptors expressed in *X. laevis* oocytes (904%). This difference in 5-hydroxyindole effect was very significant ($p < 0.0001$) and greater than the difference in 5-hydroxyindole effects obtained with GH4C1 cells transfected with either wild-type or T6'S $\alpha7$.

The Ca^{2+} fractional permeability (P_{fCa}) was investigated in the presence of 5HI, because in the absence of 5-hydroxyindole, ACh-induced Ca^{2+} transients in wild-type cells were too small to be detected. In other studies, it was demonstrated that 5-hydroxyindole does not affect P_{fCa} (Fucile et al., 2003). Simultaneous recording of I_{ACh} and the ACh-induced change of fura-2 fluorescence (Fig. 3, C and D) indicated that P_{fCa} was 7% for the T6'S mutant $\alpha7$ nAChR (Fig. 3E). For comparison, we repeated the same measurements on wild-type $\alpha7$ nAChR and found a P_{fCa} value of 8% (Table 2).

Single-Channel Conductance of T6'S Mutant $\alpha7$ Receptors. Single-channel patch-clamp experiments were conducted to identify the specific channel properties affected by the T6'S mutation. The unitary conductance is one aspect of the receptor that may have been altered with significant effect on the amount of charge carried by the mutant receptor. Therefore, to obtain high resolution single-channel currents, cell-attached patches were obtained from cells transiently transfected with the T6'S mutant. Figure 4 shows a representative recording from a cell exposed to 30 μM acetylcholine in the patch pipette. Control untransfected GH4C1 cells ($n = 6$) showed no channel openings in the presence of ACh. A current-voltage relationship was established for the T6'S mutant to quantify the single-channel conductance.

Figure 5 shows a representative current-voltage plot. Linear regression analysis gave an average slope conductance of 61.7 $\pm$ 5.8 pS. This is less than the wild-type $\alpha7$ single-channel conductance of 91.5 $\pm$ 8.5 pS previously reported (Mike et al., 2000); however, this difference might be due, at least in part, to differences in experimental solutions, because there was no extracellular magnesium and lower cal-

cium in the experiments described previously (Mike et al., 2000). In any case, it seems unlikely that the T6'S mutant has a greater single-channel conductance than wild-type $\alpha7$. This suggests that the difference in response magnitude between mutant and wild-type macroscopic currents is not attributable to a change in unitary conductance. It should be noted that although our analysis was conducted on the predominant 61.7 pS conductance, openings of lower conductance channels were sometimes observed. These smaller conductance channels were not seen in control patches, and represented no more than 16% of the total number of openings in the presence of 30 μM ACh. Furthermore, these smaller conductances were not present in all cells that responded to 30 μM ACh and only appeared in less than 20% of the total number of recordings.

Single-Channel Open Times of T6'S Mutant $\alpha7$ Receptors. Analysis of channel dwell time distributions (Fig. 6) showed that the T6'S mutant channel open times were best fit by two exponentials; the average shorter open time was 580 $\pm$ 110 μs and the longer open time was 4.3 $\pm$ 0.9 ms. Because T6'S mutant channel open times were fit by two exponential components, a weighted average was used to give an estimate of the total average open time for a macroscopic current (2.5 ms). Comparing this with the previously published apparent mean channel open time of roughly 100 μs (Mike et al., 2000) gave an increase in the channel open time of approximately 25-fold.

Burst Activity of T6'S Mutant $\alpha7$ Receptors. Figure 7A shows raw single channel events in which bursts of openings were observed under steady-state conditions. Figure 7B shows a representative closed time distribution for the T6'S mutant from patches exposed to 30 μM ACh. The requirement for multiple exponentials to fit the distribution is consistent with channel bursting. In contrast, the wild-type $\alpha7$ nAChR has been shown to have little or no burst activity under steady-state conditions (Mike et al., 2000); in other words, at the detection limits of those studies, events seemed to consist of single openings (bursts of one). In such cases, the apparent average channel open time approximated the average burst duration. However, for the currents through the T6'S mutant receptors, we could identify intraburst closures (i.e., brief gaps between sequential openings of the same single channel).

The closed time distributions of four patches that had greater than 300 events (318–6854) were best fit by four exponential components, the average time constants for which were 0.21 $\pm$ 0.03, 3.6 $\pm$ 0.4, 141 $\pm$ 40, and 2650 $\pm$ 1500 ms. Under our experimental conditions, the overall P_{open} was low, with channels open no more than 1% of the time. The P_{open} values ranged from 0.9 to 0.001% of time in the open

TABLE 2
Whole-cell voltage clamp and fractional calcium current recorded from transiently transfected GH4C1 cells
Holding potential, -70 mV. Concentration of ACh, 200 μM. Results are presented as mean $\pm$ S.E.M. The number of cells is shown in parentheses.

	nAChR	
	Wild-Type $\alpha7$	T6'S $\alpha7$
I_{ACh} (nA)	-0.06 ± 0.02 (13)*	-1.03 ± 0.36 (9)*
$I_{ACh+5HI}/I_{ACh}$ (%)	540 $\pm$ 75 (7)**	280 $\pm$ 50 (5)**
P_{fCa} (%)	8.0 $\pm$ 0.7 (10)	7.1 $\pm$ 0.6 (12)

* Significantly different (1-way analysis of variance, $P < 0.01$).
** Significantly different (1-way analysis of variance, $P < 0.05$).
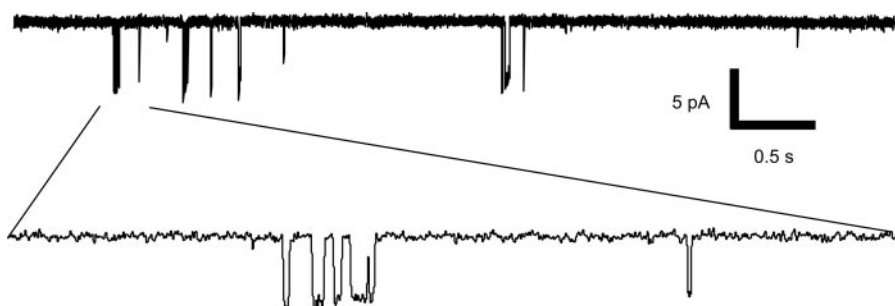

Fig. 4. Single-channel currents recorded from a GH4C1 cell expressing the T6'S mutant. Transiently transfected GH4C1 cells were studied using the cell-attached patch configuration. The representative trace shown above is from a cell with 30 μM acetylcholine in the patch pipette, at a holding potential $+$ 50 mV depolarized from resting potential. No currents were observed in untransfected control cells ($n = 6$, data not shown).

5 pA

0.5 s

state, presumably reflecting variations in the total number of channels in the patch. The two patches that had the highest frequency of openings also had a low number of simultaneous openings, accounting for 2.9 and 1.7% of the total number of events when the event frequencies were 3.8 and 1.8 events per second, respectively. As shown in Fig. 7C, the two brief time constants did not correlate to the frequency of events in the record and therefore were most likely to represent closed times associated with the reopenings of the same channel. However, the longer closed times were of greater duration when overall frequency of events was low, so that these intervals were likely to reflect the total number of channels in the patch.

Accepting just the briefest closed times as intraburst closures and using the method of Colquhoun and Sakmann (1985), a critical time value of 759 μs was determined as a threshold for defining intraburst closures. The average burst duration distributions (Fig. 8A) for the T6′S mutant defined with these criteria were best fit by two exponential components (560 $\pm$ 100 μs and 5.5 $\pm$ 1.4 ms). Histograms of the number of bursts with more than one opening were plotted and fitted by a Poisson distribution (Fig. 8B), providing a prediction of the probability of channel reopening. In this

case, the T6′S mutant had a 42.1 $\pm$ 6% probability of opening more than once.

In theory, the brief intraburst closed times ($\tau_1 = 0.21 \pm 0.03$ ms) represent time spent back in the same resting, ligand-bound, closed state that normally precedes opening (Colquhoun and Sakmann, 1985). As noted above, the closed times fit with the time constant of 3.6 $\pm$ 0.4 ms (τ_2, Fig. 7C) may also represent gaps between reopenings of the same channel. The frequency of these events was 60 $\pm$ 13% that of the briefer intraburst closures. These closures may represent times when channels close, dissociate and rebind agonist, and then reopen. On the other hand, they may represent time in a short-lived desensitized or predesensitized state (Sine and Steinbach, 1987).

Pharmacology of T6′S Mutant α7 Receptors. The concentration-response relationship for acetylcholine applied to either the T6′S mutant or wild-type α7 are shown in Fig. 9, showing a slight decrease in the apparent acetylcholine potency for the T6′S mutant compared with wild-type (see Table 3). Previous reports have shown that wild-type α7 nAChRs have significantly different peak amplitude and net charge concentration-response curves (Uteshev et al., 2002; Papke and Papke, 2002; Placzek et al., 2004). This is indic-
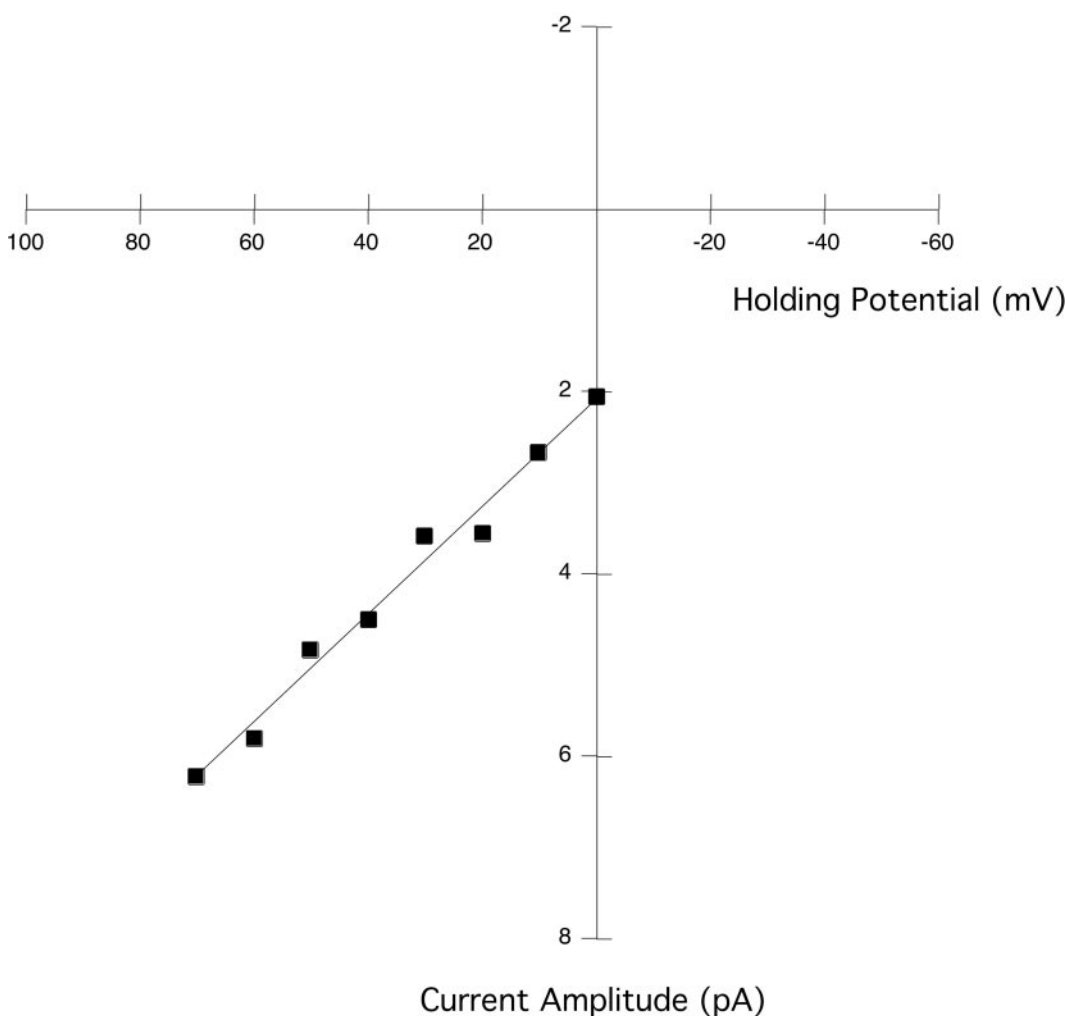

T6'S Mutant Current-Voltage Relationship

Fig. 5. The T6′S mutant α7 single-channel conductance. Single-channel current-voltage plots were generated from cell-attached patch recordings from transfected GH4C1 cells and indicated a slope conductance of 62 $\pm$ 6 pS. The data shown here are representative of those used to produce an average conductance value ($n = 5$).

ative of the strong agonist concentration dependence for the time course of their macroscopic responses. The T6′S mutant showed less of a difference between the two methods (Fig. 9B), again indicating that response kinetics are less sensitive to agonist concentration.

Agonist Selectivity Profiles. Concentration-response relationships for a series of nicotinic receptor agonists indicated that the T6′S mutant has a pharmacology that is similar to wild-type α7 with regard to both potency and efficacy of the agonists examined. Figure 10 compares the effects of several α7-selective agonists on oocytes expressing either the T6′S mutant or wild-type rat α7. Although some differences in potency and efficacy were evident, with the exception of the partial agonist tropisetron, which was nearly identical between the two receptor types (Fig. 10D), all agonists for wild-type α7 receptors tested also activated the mutant receptor. Furthermore, the potency differences observed were similar to that seen with acetylcholine (Fig. 9), suggesting a general trend in modest potency reduction for agonists. The similarity in agonist response profiles also extended to agonists that are not selective for α7-type nAChRs. The β4 subunit-selective agonist cytisine (Papke and Heinemann, 1994) and the α4β2-selective agonist metanicotine (Papke et al., 2000b) displayed agonist activity at the T6′S mutant (Table 3). Again, there was a slight reduction in potency and efficacy with the mutant, particularly in the case of cytisine, but these shifts were consistent with the general trend observed for most of the agonists examined (Table 3).

Antagonist Selectivity Profiles. Another feature of the T6′S mutant that is similar to wild-type α7 is its sensitivity to nAChR antagonists. A somewhat peculiar feature of the α7 L9′T (L248T) mutant is that several drugs that function as

antagonists of wild-type α7 have been shown to activate this mutant (Bertrand et al., 1992b; Palma et al., 1996; Demuro et al., 2001). By contrast, each of these drugs inhibited the T6′S mutant (Table 4). Furthermore, for the concentrations tested, no agonist activity of these same drugs was observed (not shown).

Discussion

Kinetic Effects of the T6′S Mutation. The mutant α7 receptor described here displayed a profound change in response kinetics, with a significant increase in responsiveness to the application of relatively high concentrations of agonist. Based on the results of receptor binding experiments, the overall increase in response magnitude observed in the T6′S mutant is apparently not due to an increase in receptor expression. This, however, is not particularly surprising, because an increase in receptor number alone would not be a likely cause of altered response kinetics. Likewise, although mutations in the pore-forming TM2 domain frequently affect single-channel conductance (Imoto et al., 1988), such a change alone would not affect the kinetics of macroscopic currents, and our data suggest that the conductance of the T6′S receptors is not substantially different from that of the wild-type.

An examination of the mean channel open time indicates that the T6′S mutant has far longer open durations than observed for wild-type α7 (Mike et al., 2000). This increased stability of the open state made it possible to record responses from cells expressing the T6′S mutant under cell-attached patch conditions. No similar data have ever been reported from wild-type α7 receptors under steady-state con-
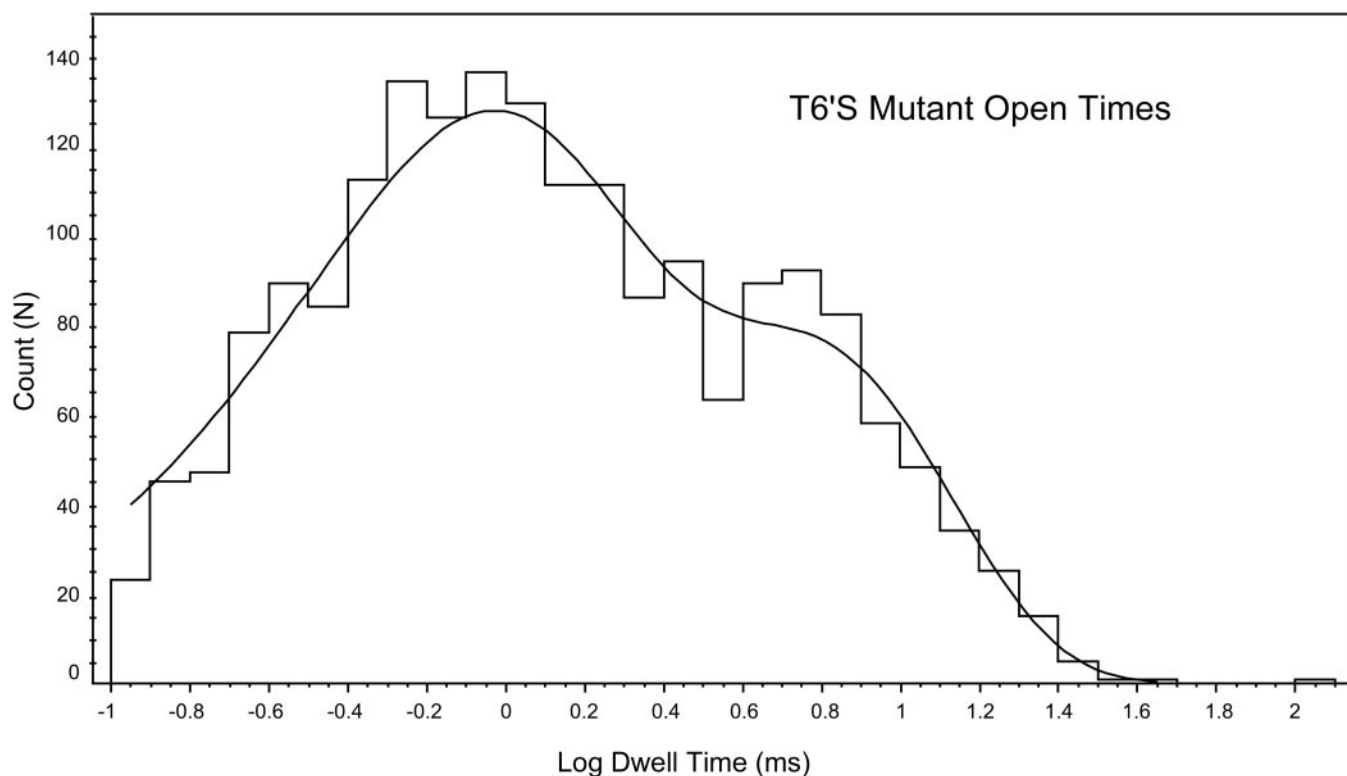

Fig. 6. T6′S single-channel open times are fit by two exponentials and indicate relatively prolonged average open times. A representative open-time distribution for a 30-min cell-attached patch recording from transfected GH4C1 cells in the sustained presence of 30 μM ACh.
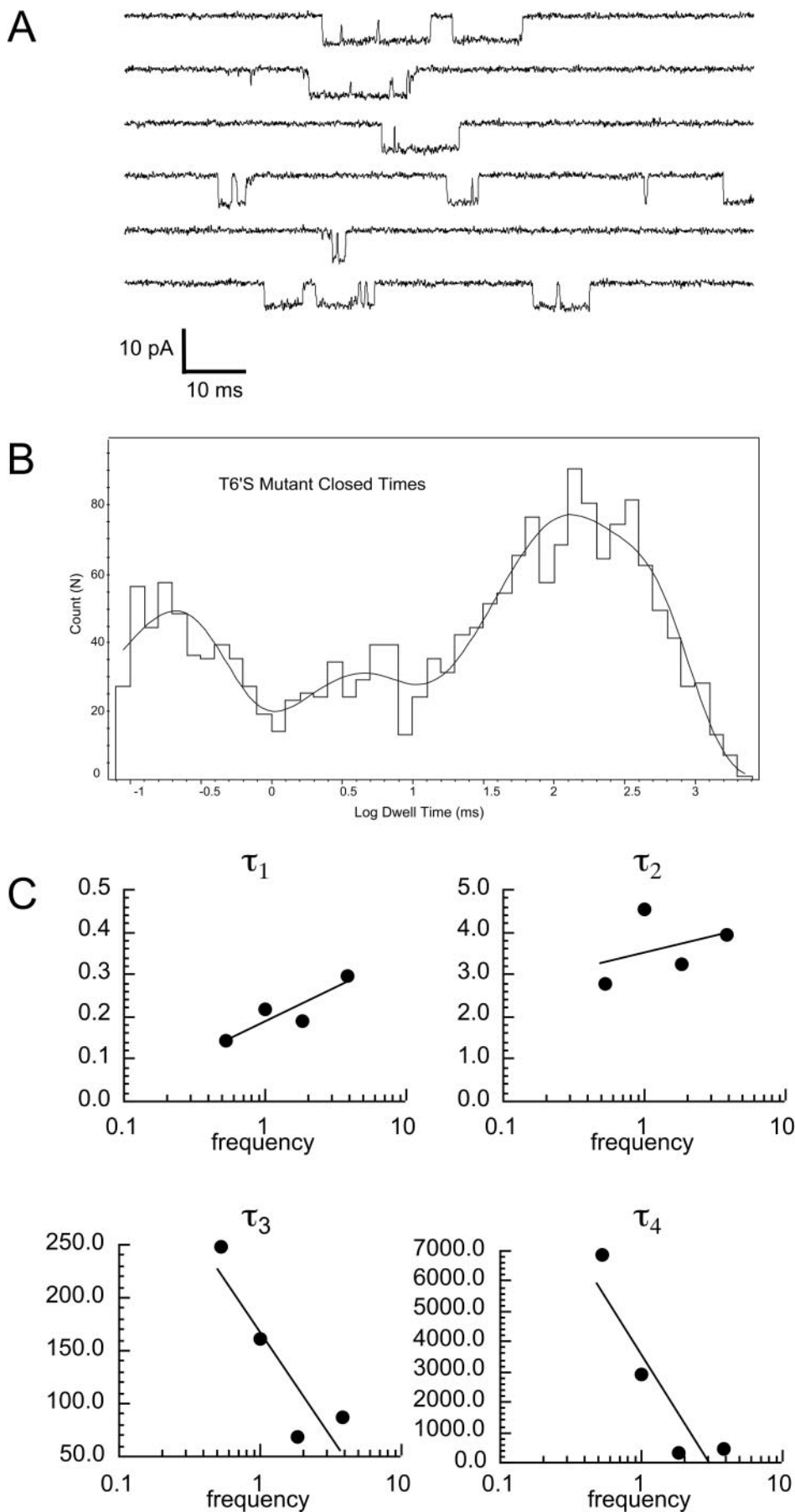
Fig. 7. T6′S mutant single-channel burst activity in transfected GH4C1 cells. A, raw data traces recorded in the presence of 30 μM acetylcholine showing channel bursts. B, closed-time distribution for the T6′S mutant showing a fit by multiple exponentials. The existence of multiple closed times is an indicator of channel bursting. To identify bursts, the critical time threshold (t_{crit}) for identifying closures within bursts was determined using the method described by Colquhoun and Sakmann (1985). C, four patches, which had between 300 and 7000 events, had event frequencies that varied from 0.5 to 3.8 events per second. The closed-time distributions from these patches were best fit with four exponential components. The time constants fit to the two briefest closed times (τ_1 and τ_2) did not vary systematically with event frequency, whereas the two slower time constants (τ_3 and τ_4) were longest when event frequency was low.

ditions of exposure to low concentrations of agonist, presumably because of the intrinsically low open probability (P_{open}) and brief lifetime of $\alpha7$-mediated single channel currents.

Burst analysis indicates that there is a significant likelihood of rapid re-opening for the T6′S mutant channel, a property not reported for wild-type $\alpha7$ channels. This in-
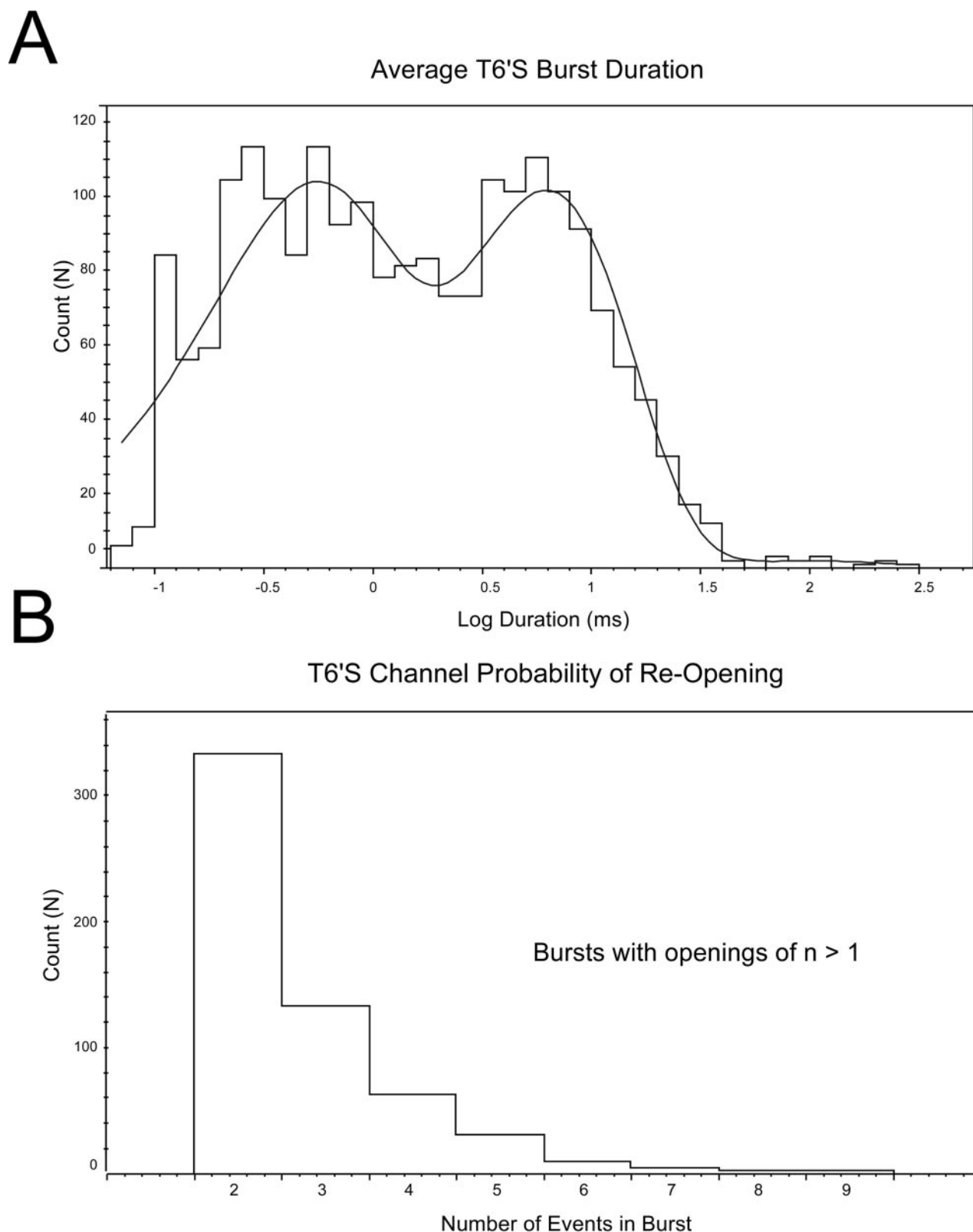
Fig. 8. T6′S mutant burst durations and number of intraburst openings recorded from transfected GH4C1 cells. A, the average burst duration distribution was best fit by two exponential components. B, the number of bursts with intraburst openings greater than unity, indicating a significant probability of the mutant channel reopening.

crease in channel reopening probably reflects a general increase in overall P_{open} for the mutant receptors. However, because no estimates were made of the number of T6′S mutant channels present in each patch, absolute P_{open} values could not be determined. Aside from the gaps associated with the rapid reopenings detected in our burst analysis, our data are not sufficient to determine whether other closed times also represent gaps between the reopenings of single channels or closed times between the independent openings of multiple channels within the patches.

In the interpretation of the kinetic effects of the T6′S mutation, there are several possible explanations for the increased macroscopic responses and prolonged responses at high agonist concentrations. We have proposed (Papke et al., 2000a) that wild-type α7 receptors are unlikely to open at high levels of agonist occupancy, and have a higher P_{open} when the multiple agonist binding sites are only partially occupied. One possibility is that one or more states that are closed in the wild-type receptor have been converted to an open state(s) in the mutant. However, our data clearly indicate that the open state itself is more stable (i.e., long-lived) in the mutant receptor than in the wild-type. This observa-

TABLE 3
Agonist profile comparison for wild-type α7 and the T6′S mutant expressed in *X. laevis* oocytes

EC_{50} values and maximum efficacy relative to acetylcholine for each of the indicated agonists.

Agonist	EC$_{50}$ (Maximum Agonist Efficacy)	
	Wild-Type α7	T6′S
	μM (%)	
ACh	30 μM (100)	100 μM (100)
Choline	300 μM (100)	2 μM (95)
GTS-21	5 μM (32)	3 μM (12)
4OH-GTS-21	1.4 μM (46)	3.3 μM (20)
AR-R17779	10 μM (78)*	30 μM (90)
Tropisetron	0.3 μM (38)†	0.9 μM (30)
Metanicotine	240 μM (16)††	400 μM (18)
Cytisine	13 μM (73)	43 μM (80)

* Potency and efficacy values derived from net charge analysis (Papke et al., 2004).
† Potency and efficacy values derived from net charge analysis (Papke et al., 2005).
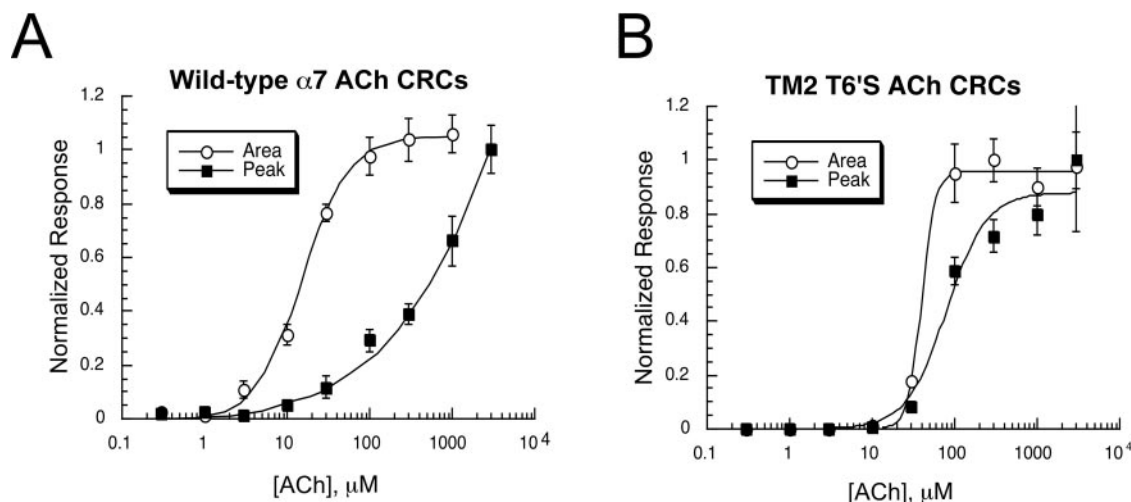†† Potency and efficacy values derived from peak CRC analysis (Papke et al., 2000b).

tion alone accounts for a large increase in P_{open} under steady-state conditions.

Wild-type α7 shows little or no apparent burst activity (Mike et al., 2000) and therefore has a probability of reopening that approaches zero. Under our experimental conditions, with 30 μM acetylcholine in the patch pipette, for the T6′S receptors the transition rates between the bound, nondesensitized states and the open states were sufficiently high relative to the dissociation and desensitization rate constants to make multiple opening bursts more likely. This indicates that the T6′S mutation alters the equilibrium between the open and activatable resting states of the receptor and the desensitized states at the level of agonist occupancy corresponding to our single-channel conditions. The fact that macroscopic currents were prolonged across the range of agonist concentrations suggests that a similar reduction or slowing of equilibrium desensitization occurs at all levels of agonist occupancy.

Although the T6′S mutation may seem to reduce agonist potency, this effect should not be interpreted outside of the context of the kinetic effects, because the apparent reduction in potency may in fact be due to a broadening of the concentration-response functions for agonists. That is, at the higher agonist concentrations that impose limitations on the responses of the wild-type receptor, the T6′S mutant showed significant increases in response. This essentially stretches out the agonist concentration-response curves (CRCs) for the mutant, producing an apparent reduction in potency.

Pharmacological Effects of the T6′S Mutation. The rapid desensitization of the wild-type α7 nAChR creates significant difficulty when attempting to study this receptor subtype, particularly in mammalian expression systems. The use of the *X. laevis* oocyte expression system circumvents this problem to some degree by providing a large cell with sufficient tolerance for application systems that are relatively slow and less likely to produce leakage. In addition, the presence of calcium-dependent chloride currents in the oocyte produces a secondary amplification of α7-mediated currents at holding potentials that are more negative than the chloride reversal potential (Miledi and Parker, 1984). Automated oocyte recording systems have been developed but, in general, have been considered medium- rather than high-

Fig. 9. Peak and area CRCs for wild-type and T6′S mutant nAChRs. Each data point represents the mean normalized response (±S.E.M.) obtained from at least four oocytes.

throughput screening systems. Truly high-throughput drug screening is best accomplished with automated systems that generate fluorescence signals and are capable of delivering hundreds of compounds in a single day to cells in multiwell plates. Because of their small transient responses, wild-type $\alpha7$ receptors are generally not suitable to use in these systems; consequently, some efforts in the area of drug discovery have attempted to make use of gain-of-function mutant $\alpha7$ receptors.

The best studied $\alpha7$ gain-of-function mutant corresponds to a change in the TM2 sequence only three amino acids away from the T6′S site [L247T in chick $\alpha7$ (Bertrand et al., 1992b) and L248T in human $\alpha7$ (Palma et al., 1999)]. Receptors with this L9′T mutation produce large nondesensitizing currents but show very unusual pharmacology compared with the wild-type $\alpha7$ nAChR. For example, several drugs have been reported to be antagonists of the wild-type receptor that are agonists of the L9′T mutant, including bicuculline, strychnine, dihydro-β-erythroidine, 5-hydroxytryptamine, hexamethonium, and tubocurarine (Bertrand et al., 1992b; Palma et al., 1996, 1999; Demuro et al., 2001). Another gain-of-function mutation (V13′T or V274T) also has pharmacological properties that are quite distinct from the wild type (Briggs et al., 1999). Although cells expressing these gain-of-function mutants can gener-

ate large signals in automated fluorescence detection systems, their failure to recapitulate the pharmacological properties of wild-type receptors, even to the point of distinguishing antagonists from agonists, limits their utility for drug screening.

One pharmacological aspect of the T6′S mutant that does differ significantly from wild-type $\alpha7$ is the reduced potentiation by 5HI. This difference was more pronounced in the oocyte studies than in the transfected cell experi-

TABLE 4
Antagonists of wild-type $\alpha7$ and their effect on the T6′S mutant expressed in *X. laevis* oocytes

Percentage reduction in peak amplitude when coapplied with 30 μM acetylcholine relative to a 30 μM acetylcholine control application. Each mean and S.E.M. represent data obtained from at least four oocytes.

Drug	Inhibition	
	Wild-type $\alpha7$	T6′S
	%	
Bicuculline, 10 μM	~63[a]	88 ± 3
5-HT, 20 μM	~25[b]	100
Tubocurarine, 1 μM	~28[c]	97 ± 2
Hexamethonium, 100 μM	100[d]	60 ± 12

[a] Demuro et al., 2001.
[b] Palma, 1996.
[c] Briggs et al., 1999.
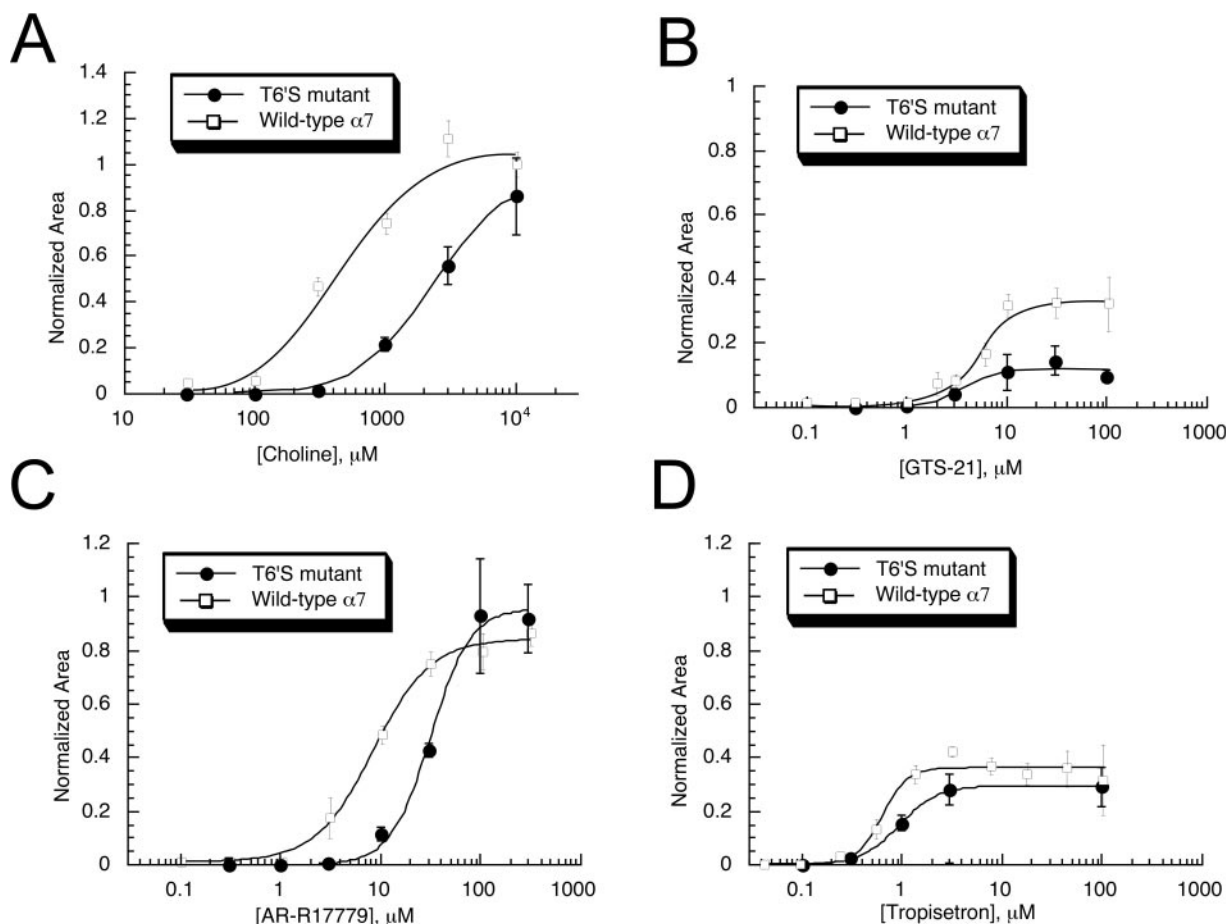[d] Bertrand et al., 1992a.

Fig. 10. Selective agonists of the wild-type $\alpha7$ nAChR. All of the agonists selective for $\alpha7$ nAChR tested, including choline (A), GTS-21 (B), AR-R17779 (C), and tropisetron (D), retained their agonist activity for the T6′S mutant. However, the concentration-response functions for the indicated drug for either wild-type $\alpha7$ or the T6′S mutant showed potency and efficacy differences, but these were relatively moderate and consistent with the potency shifts seen with non–$\alpha7$-selective and nonselective agonists, including ACh. The wild-type rat $\alpha7$ CRCs for AR-R17779 and tropisetron are taken from Papke et al. (2004) and Papke et al., (2005), respectively.

ments. This may be related to the fact that the brief ACh-evoked currents recorded in oocytes expressing wild-type α7 are augmented by transient calcium-dependent chloride currents. Whereas the T6′S receptor-mediated component of the current in oocytes may be potentiated by 5-hydroxyindole to the same degree as the currents in GH4C1 cells, there may not be a linear increase in the chloride-mediated component during the prolonged responses of the mutant channels. Because the mechanism of 5-hydroxyindole potentiation of wild-type α7 remains unknown, the reason why the T6′S receptors are less sensitive to 5-hydroxyindole than wild-type α7 receptors is unclear. It is possible that the effect of 5-hydroxyindole on the wild-type receptor is functionally similar to the effect of the T6′S mutation, in essence suggesting that the T6′S mutant is in a perpetually potentiated state. However, this explanation is not adequate to explain the observed differences. Potentiation by 5-hydroxyindole is unusual by itself, in that there is little or no effect on the macroscopic kinetics of potentiated responses compared with unpotentiated responses (Zwart et al., 2002). The fact that the T6′S mutation seems to have significant effects on the kinetics of response to agonist suggests that the mechanisms of response amplification for 5-hydroxyindole potentiation are different.

The data presented here show that the α7 T6′S mutation produces a functionally enhanced receptor that retains important characteristics of the wild-type α7 receptor, including high calcium permeability and inward rectification. The relative lack of significant changes in pharmacology indicates that this mutant receptor can prove useful in the identification of compounds that will affect α7. In support of this, the T6′S mutant expressed in *X. laevis* oocytes has recently been used to screen a panel of more than 60 compounds, and results were directly compared with those obtained with wild-type rat α7 receptors expressed in *X. laevis* oocytes (M. Bencherif, A. Placzek, R. Papke, and T. Hauser, unpublished data). The compounds tested included agonists, partial agonists, and antagonists. Activity for the mutant correlated well with that for wild-type α7. In addition, some α7 agonists, such as GTS-21, produce long-lived desensitization of wild-type α7 receptors, whereas others, such as 4OH-GTS-21 and AR-R17779, do not (Meyer et al., 1998; Papke et al., 2004). In the side-by-side comparison of 60 compounds, it was noted that the T6′S mutant was also useful to distinguish compounds that produced prolonged desensitization from those that did not (M. Bencherif, A. Placzek, R. Papke, and T. Hauser, unpublished data). These observations confirm the great potential utility of the T6′S mutant α7 for drug development.

Acknowledgments

References

Bertrand D, Bertrand S, and Ballivet M (1992a) Pharmacological properties of the homomeric alpha 7 receptor. *Neurosci Lett* **146:**87–90.

Bertrand D, Devillers-Thiéry A, Revah F, Galzi J-L, Hussy N, Mulle C, Bertrand S, Ballivet M, and Changeux J-P (1992b) Unconventional pharmacology of a neuronal nicotinic receptor mutated in the channel domain. *Proc Natl Acad Sci USA* **89:**1261–1265.

Bollmann JH, Helmchen F, Borst JG, and Sakmann B (1998) Postsynaptic Ca²⁺ influx mediated by three different pathways during synaptic transmission at a calyx-type synapse. *J Neurosci* **18:**10409–10419.

Briggs CA, McKenna DG, Monteggia LM, Touma E, Roch JM, Arneric SP, Gopalakrishnan M, and Sullivan JP (1999) Gain of function mutation of the alpha7 nicotinic receptor: distinct pharmacology of the human alpha7V274T variant. *Eur J Pharmacol* **366:**301–308.

Colquhoun D and Sakmann B (1985) Fast events in single-channel currents activated by acetylcholine and its analogues at the frog muscle end-plate. *J Physiol* **369:**501–557.

Dani JA (2001) Overview of nicotinic receptors and their roles in the central nervous system. *Biol Psychiatry* **49:**166–174.

Davies AR, Hardick DJ, Blagbrough IS, Potter BV, Wolstenholme AJ, and Wonnacott S (1999) Characterisation of the binding of [³H]methyllycaconitine: a new radioligand for labelling alpha 7-type neuronal nicotinic acetylcholine receptors. *Neuropharmacology* **38:**679–690.

Demuro A, Palma E, Eusebi F, and Miledi R (2001) Inhibition of nicotinic acetylcholine receptors by bicuculline. *Neuropharmacology* **41:**854–861.

Freedman R, Adams CE, and Leonard S (2000) The alpha7-nicotinic acetylcholine receptor and the pathology of hippocampal interneurons in schizophrenia. *J Chem Neuroanat* **20:**299–306.

Fucile S, Renzi M, Lax P, and Eusebi F (2003) Fractional Ca²⁺ current through human neuronal alpha7 nicotinic acetylcholine receptors. *Cell Calcium* **34:**205–209.

Imoto K, Busch C, Sakmann B, Mishina M, Konno T, Nakai J, Bujo H, Mori Y, Fukuda K, and Numa S (1988) Rings of negatively charged amino acids determine the acetylcholine receptors channel conductance. *Nature (Lond)* **335:**645–648.

Li Y, Papke RL, He Y-J, Millard B, and Meyer EM (1999) Characterization of the neuroprotective and toxic effects of α7 nicotinic receptor activation in PC12 cells. *Brain Res* **81:**218–225.

Meyer E, Kuryatov A, Gerzanich V, Lindstrom J, and Papke RL (1998) Analysis of 4OH-GTS-21 selectivity and activity at human and rat α7 nicotinic receptors. *J Pharmacol Exp Ther* **287:**918–925.

Mike A, Castro NG, and Albuquerque EX (2000) Choline and acetylcholine have similar kinetic properties of activation and desensitization on the alpha7 nicotinic receptors in rat hippocampal neurons. *Brain Res* **882:**155–168.

Miledi R and Parker I (1984) Chloride current induced by injection of calcium into *Xenopus* oocytes. *J Physiol* **357:**173–183.

Miller C (1989) Genetic manipulation of ion channels: a new approach to structure and mechanism. *Neuron* **2:**1195–1205.

O'Neill MJ, Murray TK, Lakics V, Visanji NP, and Duty S (2002) The role of neuronal nicotinic acetylcholine receptors in acute and chronic neurodegeneration. *Curr Drug Target CNS Neurol Disord* **1:**399–411.

Palma E, Fucile S, Barabino B, Miledi R, and Eusebi F (1999) Strychnine activates neuronal alpha7 nicotinic receptors after mutations in the leucine ring and transmitter binding site domains. *Proc Natl Acad Sci USA* **96:**13421–13426.

Palma E, Mileo AM, Eusebi F, and Miledi R (1996) Threonine-for-leucine mutation within domain M2 of the neuronal alpha7 nicotinic receptor converts 5-hydroxytryptamine from antagonist to agonist. *Proc Natl Acad Sci USA* **39:**11231–11235.

Papke RL and Heinemann SF (1994) The partial agonist properties of cytisine on neuronal nicotinic receptors containing the β2 subunit. *Mol Pharmacol* **45:**142–149.

Papke RL, Meyer E, Nutter T, and Uteshev VV (2000a) Alpha7-selective agonists and modes of alpha7 receptor activation. *Eur J Pharmacol* **393:**179–195.

Papke RL and Papke JKP (2002) Comparative pharmacology of rat and human alpha7 nAChR conducted with net charge analysis. *Br J Pharmacol* **137:**49–61.

Papke RL, Papke JKP, and Rose GM (2004) Activity of α7-selective agonists at nicotinic and serotonin receptors expressed in *Xenopus* oocytes. *BioOrg Med Chem Lett* **14:**1849–1853.

Papke RL, Schiff HC, Jack BA, and Horenstein NA (2005) Molecular dissection of tropisetron, an alpha7 nicotinic acetylcholine receptor-selective partial agonist. *Neurosci let* **378:**140–144.

Papke RL and Thinschmidt JS (1998) The correction of alpha7 nicotinic acetylcholine receptor concentration-response relationships in *Xenopus* oocytes. *Neurosci Lett* **256:**163–166.

Papke RL, Webster JC, Lippiello PM, Bencherif M, and Francis MM (2000b) The activation and inhibition of human nAChR by RJR-2403 indicate a selectivity for the α4β2 receptor subtype. *J Neurochem* **75:**204–216.

Placzek AN, Grassi F, Papke T, Meyer EM, and Papke RL (2004) A single point mutation confers properties of the muscle-type nicotinic acetylcholine receptor to homomeric α7 receptors. *Mol Pharmacol* **66:**169–177.

Quik M, Choremis J, Komourian J, Lukas RJ, and Puchacz E (1996) Similarity between rat brain nicotinic alpha-bungarotoxin receptors and stably expressed alpha-bungarotoxin binding sites. *J Neurochem* **67:**145–154.

Ragozzino D, Barabino B, Fucile S, and Eusebi F (1998) Ca²⁺ permeability of mouse and chick nicotinic acetylcholine receptors expressed in transiently transfected human cells. *J Physiol* **507:**749–757.

Rezvani AH and Levin ED (2001) Cognitive effects of nicotine. *Biol Psychiatry* **49:**258–267.

Seguela P, Wadiche J, Dinely-Miller K, Dani JA, and Patrick JW (1993) Molecular cloning, functional properties and distribution of rat brain alpha 7: a nicotinic cation channel highly permeable to calcium. *J Neurosci* **13:**596–604.

Shytle RD, Mori T, Townsend K, Vendrame M, Sun N, Zeng J, Ehrhart J, Silver AA, Sanberg PR, and Tan J (2004) Cholinergic modulation of microglial activation by alpha 7 nicotinic receptors. *J Neurochem* **89:**337–343.

Sine SM and Steinbach JH (1987) Activation of acetylcholine receptors on clonal mammalian BC3H-1 cells by high concentrations of agonist. *J Physiol* **385:**325–359.

Skok VI (2002) Nicotinic acetylcholine receptors in autonomic ganglia. *Auton Neurosci* **97:**1–11.

Sweileh W, Wenberg K, Xu J, Forsayeth J, Hardy S, and Loring RH (2000) Multistep expression and assembly of neuronal nicotinic receptors is both host-cell- and receptor-subtype-dependent. *Brain Res Mol Brain Res* **75:**293–302.

Uteshev VV, Meyer EM, and Papke RL (2002) Activation and inhibition of native neuronal alpha-bungarotoxin-sensitive nicotinic ACh receptors. *Brain Res* **948:**33–46.

Wang H, Yu M, Ochani M, Amella CA, Tanovic M, Susarla S, Li JH, Yang H, Ulloa L, Al-Abed Y, et al. (2003) Nicotinic acetylcholine receptor alpha7 subunit is an essential regulator of inflammation. *Nature (Lond)* **421:**384–388.

Webster JC, Francis MM, Porter JK, Robinson G, Stokes C, Horenstein B, and Papke RL (1999) Antagonist activities of mecamylamine and nicotine show reciprocal dependence on beta subunit sequence in the second transmembrane domain. *Br J Pharmacol* **127:**1337–1348.

Zwart R, De Filippi G, Broad LM, McPhie GI, Pearson KH, Baldwinson T, and Sher E (2002) 5-Hydroxyindole potentiates human alpha 7 nicotinic receptor-mediated responses and enhances acetylcholine-induced glutamate release in cerebellar slices. *Neuropharmacology* **43:**374–384.

Address correspondence to: Roger L. Papke, Department of Pharmacology and Therapeutics, P. O. Box 100267, University of Florida, Gainesville, FL 32610-0267. E-mail: rlpapke@ufl.edu